International Association for Hydro-Environment Engineering and Research
Supported by Spain Water and IWHR, China

Proceedings of the 8th International Symposium on Environmental Hydraulics (ISEH 2018)
4 -7 June 2018, University of Notre Dame, Indiana, USA

CONTINUOUSLY FED DENSITY CURRENTS OVER POROUS BED

VENULEO SARA[(1)], SCHLEISS ANTON[(1)] & FRANCA MÁRIO J.[(2)]

[(1)] École polytechnique fédérale de Lausanne, Lausanne, Switzerland, sara.venuleo@epfl.ch

[(2)] IHE Delft Institute for Water Education, Delft, The Netherlands, m.franca@un-ihe.org

ABSTRACT

Gravity currents impact significantly the environment and human's life. Understanding their internal structure and their dynamics is fundamental for modelling purposes. In this study we observe experimentally how bed porosity affects the dynamics of density currents. We will focus on density and velocity profiles of currents traveling over porous bed, sinking and entraining water from its cavities. This abstract presents the preliminary results of this study which are relative to density currents travelling over the reference substratum, a smooth impermeable bed. The tests presented will be used as a reference to observe how the water entrained from the bottom cavities can change the structure of the current and are herein used to validate the experimental techniques. Brine water is injected at constant discharge in a 7.5 m long, 0.3 m wide and 0.3 m deep flume while instantaneous velocity and density profiles are simultaneously acquired 3 m downstream of the inlet. Initial excess densities and inlet velocities allow to reproduce gravity flows in sub and super-critical regime.

Keywords: density currents, Densimetric Froude number, velocity and density profiles, porous bed, bottom water entrainment

1. INTRODUCTION

Density or gravity currents are geophysical flows driven by the density differences between two contacting fluids which can be caused by temperature differences, presence of dissolved substances (i.e. salt) or presence of particles in suspension. Desalinization plants overflows, oil spillage release in the ocean, turbidity currents yielding deposition in reservoirs, airborne snow avalanches and oceanic currents are, among others, examples of the impact of gravity currents on human life and on the environment.

The importance of these phenomena and of their related effects explains the large number of theoretical, experimental and numerical studies existing on gravity currents. The vertical structure of gravity flows has been experimentally studied over smooth and rough bed by many authors (Stagnaro and Bolla Pittaluga 2014; Sequeiros et al. 2010; Kneller, et al. 1999; among others).

Several studies about gravity currents propagating over porous beds also exist. However most of the existing studies concern viscous gravity flows (Zheng et al. 2015; Pritchard and Hogg 2002; Acton et al. 2001; among others). Results concerning inertial gravity currents mainly deal with lock-exchange gravity currents (Thomas and Marino 2012; Thomas et al. 2004, 1998) whose dynamics depend on non-always-physically meaningful length scales, like the length of the lock, the length of the channel (influencing the timing of the different current phases) or the initial lock-water-depth.

In the present study we assess the influence of bed porosity on the structure of an inertial continuously-fed gravity current. Particularly we aim at characterizing the current density and velocity profiles.

Results presented hereafter only refer to tests performed over smooth bed. These are used as reference to observe the effect of clear water incorporation from the bottom porosities on the current vertical structure and dynamics and also to validate the experimental setup.

2. EXPERIMENTAL METHODS

The experiments are carried out in a 7.5 m long, 0.3 m wide and 0.3 m deep horizontal flume initially filled with 0.2 m of clear water having density 1000.8 kg/m^3. Its smooth, horizontal bottom has a 0.2 m deep, 1 m long, hollow placed 3 m downstream the inlet. This cavity is filled with different arrangements of sticks simulating bed of different porosities. The results here reported are obtained filling completely the mentioned cavity so that the bottom is impermeable and smooth. Brine water of known density is injected at constant rate at the upstream extremity of the channel, through a 0.28m wide and 0.06 m high inlet section. A continuously fed density current forms and travels along the channel finally sinking into a reservoir located at the downstream extremity of the channel where the water level is kept constant thanks to the presence of a weir. The facility is represented in Figure 1.

At 3 m downstream of the inlet, instantaneous 3D velocity profiles are acquired through an Acoustic Doppler Velocity Profiler (ADVP) whose special configuration (one emitter and four receivers) allows to eliminate signal noise and to check the data quality. Simultaneously a 2D width-averaged image of the current is acquired with a high speed camera placed perpendicularly to the channel sidewalls, in correspondence of the ADVP acquisition profile. A known amount of fluorescent ink is added to the brine water injected into the channel so that an image analysis technique, based on ink-light absorption and similar to the one applied by Nogueira et al. (2013) and Hacker et al. (1996) and allows to assess the instantaneous two-dimensional density field (see Figure 2).

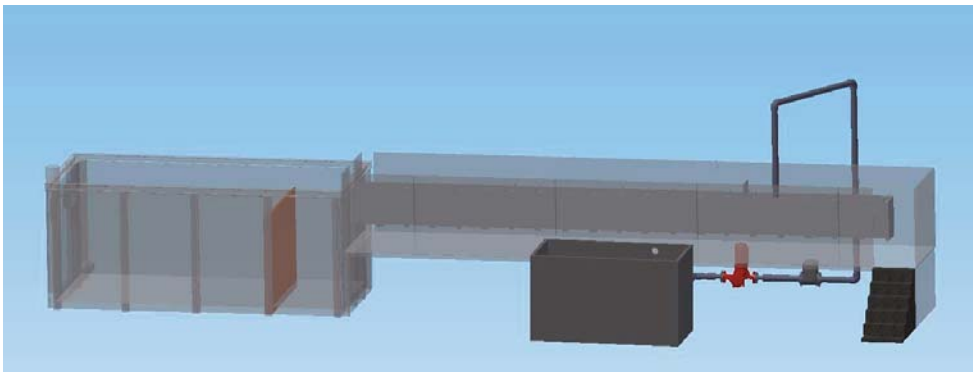

Figure 1. Representation of the facility.

The density of the injected brine water and the inlet discharge are changed at each experience to observe currents in sub and super-critical regimes. Table 1 summarizes the initial conditions of the tests and the corresponding inlet Froude (FR_I) and Reynolds (Re_I) numbers computed according to Equation [1] and [2]:

$$FR_I = \frac{v_I}{\sqrt{(\rho_I - \rho_0)/\rho_0 \cdot g \cdot h_I}} \quad [1]$$

$$\mathrm{Re}_I = \frac{\rho_I h_I v_I}{\mu_I} \quad [2]$$

Note that, travelling downstream, the current characteristic density, velocity and depth change and with them the current Froude and Reynolds numbers evolve reaching a sort of equilibrium value. These values are hereafter referred to as FR_c and Re_c and are computed according to equation [3] and [4]:

$$FR_c = \frac{\langle v \rangle_h}{\sqrt{\langle \Delta\rho \rangle_h / \rho \cdot g \cdot h}} \quad [3]$$

$$\mathrm{Re}_C = \frac{\langle \rho \rangle_h h \langle v \rangle_h}{\mu} \quad [4]$$

where the symbol $\langle \theta \rangle_h$ is the current depth-averaged value of a flow variable (being Z_I the current interface):

$$\langle \theta \rangle = \frac{1}{h} \int_0^{z_I} \theta \, dz \quad [5]$$

In the following Z_I is identified applying a threshold value to the density. Following Hacker et al. (1996) the current depth is identified applying a density threshold equal to the ambient water density plus 10% of the initial excess density.

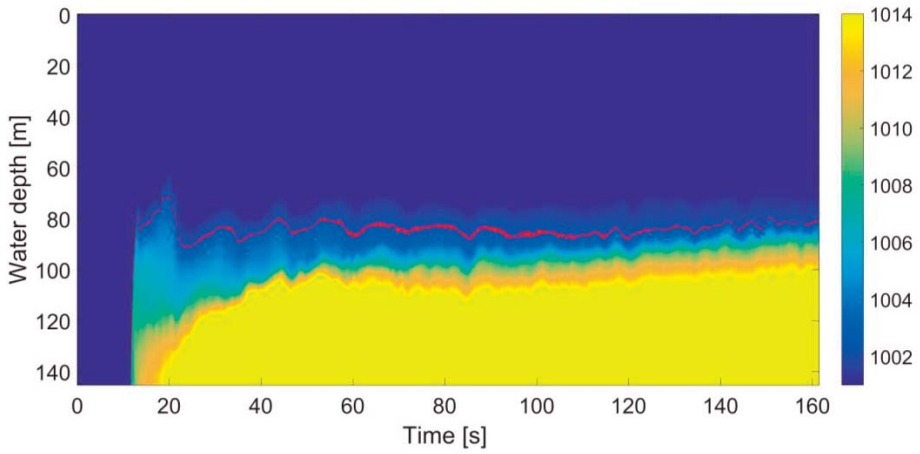

Figure 2: Time evolution of width-averaged density in the profile of interest. The red line marks the iso-contour corresponding to the applied density threshold (ambient water density plus 10% of the initial excess density)

Table 1. Summary of the test initial conditions

	EXCESS DENSITY (KG/M^3)	INLET VELOCITY (M/S)	INLET FROUDE NUMBER	INLET REYNOLDS NUMBER
TEST 1007	1007	0.072	1.19	3103
TEST 1014	1014	0.072	0.83	3124

3. RESULTS

3.1 Head advancement velocity

The head advancement velocity is assessed by both, the video analysis and the ADVP velocity measurements. As expected, having equal inlet velocity but different initial excess density, the two tests show different head advancing velocity: respectively 75.7 mm/s (for TEST1 ρI= 1007 Kg/m^3) and 119.4 mm/s (for TEST2 ρI= 1014 Kg/m^3). The head velocity is constant in the measuring window (having length 0.28 m).

3.2 Current depth

The two currents show a similar evolution of current-depth (see Figure3 showing the current depth evolution in time in correspondence of the ADVP measurement profile), characterized by a sudden rise in correspondence of the head after which the current depth-occupation decreases to its minimum value. This minimum is followed by a progressive increase in current depth lasting about 25 seconds, after which the current depth stabilizes and fluctuates around a constant value which remains steady during the entire current-body transition. Time t = 0 s in Figure 3 refer to the instant in which the current enters the measuring window.

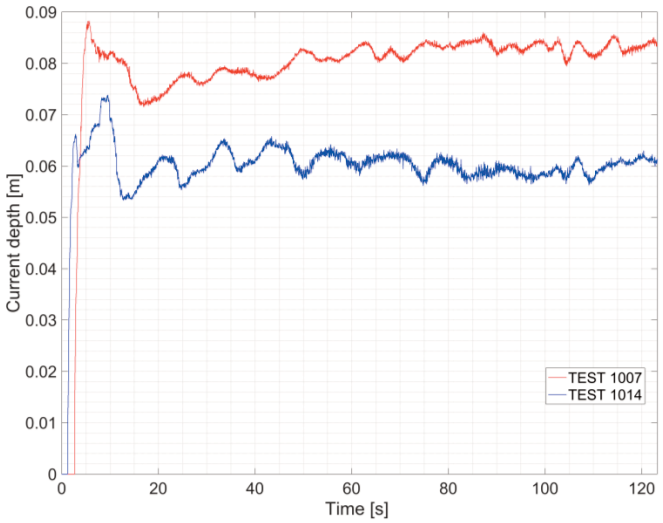

Figure 3. Current depth evolution in time in correspondence of the ADVP measurement profile.

3.3 Dimensionless current parameters

The Densimetric Froude number of the current evolves in time and space. To characterize the two tests we consider its value in correspondence of the profile located in the middle of the measuring window, where both velocity and density measures are available. After a transient period its value stabilizes and fluctuates around a constant value, as current depth, current depth averaged velocity and depth averaged density do. Indeed looking at the current depth evolution (see Figure 3), after the head and transition zone, it is possible to recognize (more or less in correspondence of t = 60 s) the beginning of a quasi-steady flow know as body of the current. During this phase the Densimetric Froude number value, computed using the depth averaged flow variables values (i.e. according to equations [3] and [4]), is 1.08 for TEST 1007 and 0.86 for TEST 1014. The current Reynolds number in the section of interest, instead, is computed to be 3699 and 3114 for TEST 1007 and TEST 1014 respectively.

3.4 Body time averaged density and velocity profiles

Figure 4 represents the time average of the density profile in the section of interest normalized by the initial excess density, during the body transition. The density is constant and close to the value of the initial injected water density over 25% of the water depth for TEST 1014 and over 40% of water depth for TEST 1007. The mixing layer occupies from 25 to 30% of the current depth in both cases.

3.5 Water entrainment at the upper boundary

To evaluate entrainment, the parametrization developed by Cenedese et al. (2010) was used. Indeed the one proposed by Ellison and Turner (1959) is only valid when the Densimetric Froude number Fr_c is greater than 1.12 which is not the case for our tests. Using the values of Re_c and FR_c computed in Paragraph 3.3, we obtained E=0.0054 for TEST 1007 and E=0.0012 for TEST 1014 respectively; where E is the proportionality constant between the depth-averaged velocity and the

entrainment velocity. Considering the entrainment velocity as the velocity normal to the interface of the current we computed E to be 0.0085 and 0.005 respectively for TEST 1007 and TEST 1014. These values are similar to the ones given by Cenedese et al. (2010) parametrization.

4. CONCLUSIONS

We showed some of the preliminary results obtained reproducing experimentally continuously-fed density currents flowing over smooth bed. Two tests having different initial excess density and Densimetric Froude number are presented. Given that the obtained results are meaningful, the experimental set up has proved to be adequate for its purpose. These results will be compared with the ones obtained over porous bed to assess the effect of the bottom porosity on the vertical structure of the current. Particularly we are interested in observing how density and velocity profiles are affected by the water entrained from the bottom cavities.

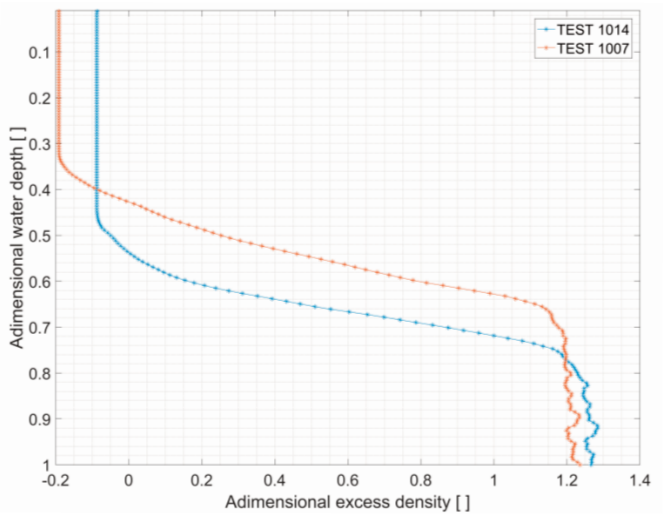

Figure 4. Time averaged dimensionless excess density profile in the section of interest during the current-body transition.

ACKNOWLEDGMENTS

The first author acknowledges support from the Swiss National Science Foundation (SNSF Grant Number: 200021 159249).

REFERENCES

Acton J. M., Huppert H. E., and Worster M. G. (2001). Two-Dimensional Viscous Gravity Currents Flowing over a Deep Porous Medium. *Journal of Fluid Mechanics*, 440.

Cenedese C., and Adduce C. (2010). A New Parameterization for Entrainment in Overflows. *Journal of Physical Oceanography*, 40 (8), 1835–50.

Ellison T. H., and Turner J. S. (1959). Turbulent Entrainment in Stratified Flows. *Journal of Fluid Mechanics*, 6 (03), 423–448.

Hacker J., Linden P.F., and Dalziel S.B. (1996). Mixing in Lock-Release Gravity Currents. *Dynamics of Atmospheres and Oceans,* 24, 183-195.

Kneller B.C., Sean J. B., and McCaffrey W.D. (1999). Velocity Structure, Turbulence and Fluid Stresses in Experimental Gravity Currents. *Journal of Geophysical Research: Oceans*, 104 (C3), 5381–91.

Nogueira H.I.S, Adduce C., Alves E., and Franca M.J. (2013). Image Analysis Technique Applied to Lock-Exchange Gravity Currents. *Measurement Science and Technology,* 24 (4), 047001.

Pritchard D., and Hogg A.J. (2002). Draining Viscous Gravity Currents in a Vertical Fracture. *Journal of Fluid Mechanics*, 459.

Sequeiros O.E., Spinewine B., Beaubouef R.T., Sun T., Garcia M.H., and Parker G. (2010). Characteristics of Velocity and Excess Density Profiles of Saline Underflows and Turbidity Currents Flowing over a Mobile Bed. *Journal of Hydraulic Engineering,* 136 (7), 412–433.

Stagnaro M., and Bolla Pittaluga M. (2014). Velocity and Concentration Profiles of Saline and Turbidity Currents Flowing in a Straight Channel under Quasi-Uniform Conditions. *Earth Surface Dynamics*, 2 (1), 167–80.

Thomas L. P., and Marino B. M. (2012). Inertial Density Currents over Porous Media Limited by Different Lower Boundary Conditions. *Journal of Hydraulic Engineering,* 138 (2): 133–42.

Thomas L. P., Marino B. M., and Linden P. F. (1998). Gravity Currents over Porous Substrates. *Journal of Fluid Mechanics,* 366, 239–58.

Thomas L. P., Marino B. M., and Linden P. F. (2004). Lock-Release Inertial Gravity Currents over a Thick Porous Layer. *Journal of Fluid Mechanics,* 503, 299–319.

Zheng Z., Shin S., and Stone H.A. (2015). Converging Gravity Currents over a Permeable Substrate. *Journal of Fluid Mechanics*, 778, 669–90.